Contents lists available at ScienceDirect

Molecular Immunology

Prothymosin α immunoactive carboxyl-terminal peptide TKKQKTDEDD stimulates lymphocyte reactions, induces dendritic cell maturation and adopts a β-sheet conformation in a sequence-specific manner

Margarita Skopeliti [a,*], Vassiliki A. Iconomidou [b], Evelyna Derhovanessian [c], Graham Pawelec [c], Wolfgang Voelter [d], Hubert Kalbacher [d,e], Stavros J. Hamodrakas [b], Ourania E. Tsitsilonis [a,*]

[a] Department of Animal and Human Physiology, Faculty of Biology, University of Athens, Athens, Greece
[b] Department of Cell Biology and Biophysics, Faculty of Biology, University of Athens, Athens, Greece
[c] Center for Medical Research, Tuebingen Ageing and Tumor Immunology Group, University of Tuebingen, Tuebingen, Germany
[d] Institute of Physiological Chemistry, University of Tuebingen, Tuebingen, Germany
[e] PANATecs, Tuebingen, Germany

ARTICLE INFO

ABSTRACT

Prothymosin α (ProTα) is a small acidic polypeptide with important immunostimulatory properties, which we have previously shown to be exerted by its carboxyl (C)-terminus. It exerts immunoenhancing effects through stimulation of monocytes *via* toll-like receptor (TLR) triggering. Here, we assayed the activity of synthetic peptides homologous to ProTα's C-terminus to stimulate lymphocyte functions, in particular natural killer cell cytotoxicity of peripheral blood mononuclear cells isolated from healthy donors. A synthetic decapeptide TKKQKTDEDD was identified as the most potent lymphocyte stimulator. The activity of this peptide was sequence-specific and comparable to that of the intact molecule, suggesting that ProTα's immunoactive segment encompasses the nuclear localization signal sequence of the polypeptide. Because ProTα stimulates immune responses in a monocyte-dependent manner, we further investigated whether the entire molecule and its peptide TKKQKTDEDD specifically act on monocytes and show that both can promote maturation of monocyte-derived dendritic cells (DC). Finally, knowing that, under specific conditions, ProTα forms amyloid fibrils, we studied the amyloidogenic properties of its C-terminal peptide segments, utilizing ATR FT-IR spectroscopy and transmission electron microscopy (negative staining). Although the peptide TKKQKTDEDD adopts an antiparallel β-sheet conformation under various conditions, it does not form amyloid fibrils; rather it aggregates in globular particles. These data, in conjunction with reports showing that the peptide TKKQKTDEDD is generated *in vivo* upon caspase-cleavage of ProTα during apoptosis, strengthen our hypothesis that immune response stimulation by ProTα is in principle exerted *via* its bioactive C-terminal decapaptide, which can acquire a sequence-specific β-sheet conformation and induce DC maturation.

© 2008 Elsevier Ltd. All rights reserved.

1. Introduction

Prothymosin α (ProTα) is a glutamic-rich, 109 amino acid (aa) residue long polypeptide (Haritos et al., 1984), principally located in the cell nucleus (Manrow et al., 1991). ProTα is highly conserved among mammals and ubiquitously expressed in all tissues (Haritos, 1987), at levels in excess of 10,000 copies per cell (Eschenfeldt and Berger, 1986). This high level of expression suggests ProTα's participation in important cellular molecular circuits. Ample experimental evidence highlights the crucial role of ProTα in cell survival and proliferation. With respect to the latter, it has been shown that ProTα regulates DNA remodelling during proliferation (Díaz-Jullien et al., 1996) and modulates nuclear processes by directly interacting with free-core histone H1 (Gomez-Marquez et al., 1989; Karetsou et al., 2002). In addition, ProTα regulates apoptosis through prevention of apoptosome formation (Jiang et al., 2003), while being itself an early target of activated caspase-3 (Enkemann et al., 2000). In cells undergoing apoptosis, ProTα cleavage by caspases generates a carboxyl (C)-terminally truncated

polypeptide (aa 1–99), which sequesters cytochrome C (Markova et al., 2003).

Initially isolated from rat thymus (Haritos et al., 1984), ProTα was so-named as the precursor polypeptide of thymosin α1-related peptides and was believed to be the main molecule responsible for the immmunostimulatory capacity of the thymic extract, thymosin fraction 5. Since 1984, studies on ProTα attributed significant immunoenhancing properties to the polypeptide, leading to its classification in the broad family of biologic response modifiers (Pan et al., 1986). Thus, in *in vitro* experiments, ProTα enhances T-cell proliferation in response to cellular antigens (Baxevanis et al., 1988), increases monocyte HLA-DR molecule expression (Baxevanis et al., 1992), amplifies natural killer (NK) cell cytotoxicity *via* induction of perforin production and integrin expression (Skopeliti et al., 2006; Voutsas et al., 2000) and augments hydrogen peroxidase-mediated neutrophil antimicrobial responses (Heidecke et al., 1997). ProTα's immunoactivity is reported to be even more pronounced on lymphocytes of patients with malignancies (Eckert et al., 1997; Garbin et al., 1997) or autoimmune diseases (Reclos et al., 1987) *in vitro* and most importantly, it can potentiate the deficient responses of immunosuppressed or tumor-bearing animals *in vivo* (Haritos, 1987; Papanastasiou et al., 1992). These data suggest that its application may be of benefit in clinical protocols.

Investigating the molecular mechanisms responsible for ProTα's activity, recent data from our group suggest that its immunologically active segment is located at the C-terminus of the polypeptide, spanning the sequences aa(89–102) and aa(103–109) (Skopeliti et al., 2006). Therefore, it seems that different parts of the molecule are responsible for ProTα's dual mode of action, the central, energy-rich histone-binding region spanning aa(52–82) for its intracellular/proliferative role (Papamarcaki and Tsolas, 1994) and the C-terminal region aa(89–109) for its extracellular/immunomodulating function (Skopeliti et al., 2006). Moreover, *via* proteomic analysis we were able to provide evidence that ProTα's immune effect is exerted *via* toll-like receptor (TLR) signaling (Skopeliti et al., 2007). Interestingly, this information supplemented previous results supporting ProTα's monocyte-dependent mode of action in unfractionated peripheral blood mononuclear cell (PBMC) cultures (Voutsas et al., 2000), as well as its activity on cells of both the innate (e.g. macrophages, neutrophils, NK cells) (Cordero et al., 1995; Heidecke et al., 1997; Papanastasiou et al., 1992) and the adaptive arms of immunity (e.g. CD4+ and CD8+ T-cells) (Voutsas et al., 2000).

In the context of these pleiotropic activities, here we aimed to elucidate ProTα's immune-related mechanism of action underlying its immunoenhancing properties. First, in order to identify the exact sequence comprising the 'immunological core' of ProTα, we assessed the activity of prolonged synthetic peptides, homologous to the polypeptide's C-terminus. Second, given that ProTα acts on monocytes *via* TLR, we investigated the causal connection between monocyte stimulation with ProTα or its active peptide and their subsequent maturation into competent dendritic cells (DC). Finally, we sought to explore the structural characteristics of ProTα and its active peptide attributing their activity to a specific secondary conformation.

2. Materials and methods

2.1. Peptide synthesis

Peptides were synthesized by the Fmoc (9-fluorenylmethoxycarbonyl)/tBu chemistry utilizing a multiple peptide synthesizer Syro II (MultiSynTech, Witten, Germany). After cleavage, crude peptides were purified by HPLC on a reverse phase C18 Nucleosil 100-5C column (HPLC Technologies, UK) to a purity of >95%, using a linear gradient of 5–80% acetonitrile in 0.05% trifluoroacetic acid for 45 min. All peptides were characterized by matrix-assisted laser desorption ionization-time of flight mass spectrometry and results were in all cases in agreement with the calculated masses.

2.2. PBMC isolation

Leukocyte-rich buffy coats were prepared from healthy blood donors (through the courtesy of Dr. A. Karafoulidou, Blood Transfusion Unit, Athens General Hospital 'Laikon', Athens, Greece). PBMC were isolated over lymphocyte separation medium (PAA Laboratories GmbH, Pasching, Austria) density gradient centrifugation and cultured in RPMI-1640 with Glutamax (Cambrex BioScience, Verniers, Belgium), supplemented with 10% heat-inactivated fetal bovine serum (FBS) (Cambrex), 50 μg/ml garamycin (Cambrex), 10 mM Hepes (Cambrex) and 50 μM 2-mercaptoethanol (Sigma–Aldrich Chemie GmbH, Munich, Germany) at a concentration of 1×10^6 cells/ml, in a humidified atmosphere at 37 °C, 5% CO_2.

2.3. NK cell activity

PBMC were activated in the presence of pretitrated (Baxevanis et al., 1999) concentration of ProTα (160 ng/ml) or its C-terminal synthetic peptides (25 ng/ml) synergistically with low-dose (20 IU/ml) recombinant human (rh) IL-2 (Cetus Corp., Los Angeles, CA) in 24-well plates (Greiner Bio-One International AG, Frickenhausen, Germany). Following a 3-day incubation at 37 °C, 5% CO_2, cells were harvested and tested as effectors (E) against the tumor target (T) cell lines K562 (chronic myelogenous leukemia; NK-sensitive) and Daudi (Burkitt's lymphoma; NK-resistant) in standard ^{51}Cr-release cytotoxicity assays. Target cells were ^{51}Cr-labelled for 1 h at 37 °C in the presence of 3.7 MBq of Na^{51}CrO$_4$ (Amersham Biosciences Ltd., Buckinghamshire, UK) in 20% FBS-enriched RPMI culture medium and washed three times to minimize non-stably incorporated, spontaneous radioisotope release. E and T cells were co-cultured in quadruplicate, in U-bottom 96-well microtiter plates (Greiner) at a ratio of 40:1 for 18 h at 37 °C. At the end of the incubation period, 100 μl of supernatant was removed from each well and isotope release was counted in a γ-counter (1275 Minigamma, LKB Wallac, Turku, Finland). To determine maximal and spontaneous isotope release, targets were incubated with 3N HCl and in complete medium alone, respectively, the latter not exceeding 15% of maximal release in any experiment. Percentage of specific cytotoxicity was calculated according to the formula: (cpm experimental − cpm spontaneous)/(cpm maximal − cpm spontaneous) × 100. The experiment was performed utilizing 12 healthy donor-derived PBMC cultures.

2.4. DC generation and maturation

Highly enriched monocytes (>80% CD14+) were obtained from PBMC of 8 healthy volunteers by plastic adherence for 2 h at 37 °C. Non-adherent cells were removed after three washing steps, and thereafter monocytes ($1–2 \times 10^6$/ml) were cultured in 6-well plates (Greiner) for 6 days in X-VIVO-15 medium (Cambrex) supplemented with 800 IU/ml rhGM-CSF and 500 IU/ml rhIL-4 (both from R&D Systems GmbH, Wiesbaden-Nordenstadt, Germany). On day 6, non-adherent immature DC (iDC) were rinsed off, washed once in PBS and plated in new 6-well plates. At this time-point, iDCs were cultured with ProTα (160 ng/ml), its C-terminal peptides (25 ng/ml) or LPS (5 ng/ml; Sigma–Aldrich) as a positive control. Cells were recovered after 24–48 h culture for flow cytometric analysis.

2.5. Phenotypic analysis

iDC and mature DC were harvested and stained for HLA-DR, CD80, CD83, CD86, CD11b, CD40 and CD14 molecule expression. Triple staining was performed using FITC-, PE- or Cy5-labelled mouse anti-human IgG1 monoclonal antibodies (mAb; Becton Dickinson Biosciences, Erembodegem, Belgium) at saturating concentrations for 30 min on ice. In parallel, harvested cells were also stained with unrelated FITC-, PE- and Cy5-conjugated anti-human IgG1 mAb, as isotype controls. Flow cytometric data of $1–2 \times 10^4$ total cells acquired with an LSR-II flow cytometer (Becton Dickinson) were analysed using CellQuest software.

2.6. Attenuated total reflectance Fourier-Transform Infrared (ATR FT-IR) spectroscopy and post-run spectra computations

Five-microliter drops of the ProTα's C-terminal synthetic peptide suspensions (5 mg/ml) were cast on flat stainless-steel plates coated with an ultrathin hydrophobic layer (SpectRIM, Tienta Sciences, Inc. Indianapolis, USA) and left to air-dry slowly at ambient conditions to form thin films. IR spectra were obtained at a resolution of $4 \, cm^{-1}$, utilizing an IR microscope (IRScope II, BrukerOPTICS, Bruker Optik GmbH, Ettlingen, Germany), equipped with a Ge ATR objective lens ($20\times$) and attached to a FT spectrometer (Equinox 55, BrukerOPTICS). Ten 32-scan spectra were collected from each sample and averaged to improve the S/N ratio. All spectra are shown in the absorption mode after correction for the wavelength-dependence of the penetration depth (d_p analogous λ). Absorption band maxima were determined from the minima in the second derivative of the corresponding spectra. Derivatives were computed analytically using routines of the OPUS/OS2 software after a 13 point smoothing around each data point, by the Savitsky–Golay algorithm (Savitsky and Golay, 1964). Smoothing over narrower ranges resulted in deterioration of the S/N ratio and did not increase the number of minima that could be determined with confidence.

2.7. Transmission electron microscopy (negative staining)

For negative staining, 3 μl of ProTα aa(100–109) peptide suspension (5 mg/ml) were applied to glow-discharged 400 mesh carbon-coated copper grids for 60 s. The grids were stained with a drop of 1% (w/v) aqueous uranyl acetate for 45 s. Excess stain was removed by blotting with a filter paper and the grids were left to air-dry. The grids were examined in a Philips CM10 electron microscope operated at 100 kV. Photographs were obtained by a retractable slow scan CCD camera (Gatan Inc.) utilizing the Digital Micrograph Software package (Gatan Inc.).

2.8. Statistical analysis

The data were analysed by the Student's t-test and statistical significance was presumed at significance level of 5% ($p < 0.05$).

2.9. Modelling

The antiparallel β-pleated sheet model was built by extracting from the PDB (Berman et al., 2000) hairpins with sequences that resembled the ProTα peptide sequence motif as closely as possible. The model was converted by homology modelling into the ProTα peptide antiparallel β-sheet model, utilizing the WHAT IF (Vriend, 1990) program. The PyMOL (DeLano, 2002) program was used to produce ribbon diagrams of the model.

3. Results

3.1. Identification of the active peptide segment (TKKQKTDEDD) of ProTα

Previous data support the localization of ProTα's immunoreactive fragment at the C-terminus of the polypeptide, specifically within the sequences aa(89–102) and aa(103–109) (Skopeliti et al., 2006). This was the first indication that ProTα's immunological role can be attributed to the activity of a defined segment, immunologically overlooked to date and considered important only for the polypeptide's nuclear targeting (Manrow et al., 1991). In the present study, we sought to precisely define the C-terminal area responsible for immune stimulation.

To this end, we synthesized a series of C-terminal peptides spanning ProTα's sequence aa(103–109) to aa(94–109) (Table 1), as well as the amino (N)-terminal peptide aa(1–28), known as thymosin α1 (Tα1) and reported to be of immunological significance (Haritos, 1987). The activity of these synthetic peptides was evaluated through their ability to enhance, to levels comparable to the intact polypeptide, non-MHC restricted PBMC cytolytic activity. Knowing that ProTα acts synergistically with suboptimal doses of IL-2 to optimally augment NK and lymphokine-activated killer (LAK) cell cytotoxicity (Lopez-Rodriguez et al., 1994; Voutsas et al., 2000), PBMC effector responses were measured after 3-day activation with ProTα or the synthetic peptides in combination with low concentrations of IL-2 (20 IU/ml). Median NK cell activity, as tested against K562 targets, showed that the peptides aa(103–109), aa(102–109), aa(101–109), aa(100–109) and aa(99–109), increased the percentage of NK-derived specific lysis of K562 cells to 32.7%, 25.2%, 27.8%, 35.3% and 32.4%, respectively. This increase was statistically significant ($p < 0.05$) compared to the effect induced by low IL-2 dose (10.6%) and similar to the effect of ProTα and IL-2 (38.1%; Fig. 1). Analogous results were observed when testing the same PBMC' LAK lytic activity against Daudi targets: peptides aa(103–109), aa(102–109), aa(101–109), aa(100–109) and aa(99–109) increased cytotoxicity to 36.9%, 35.9%, 31.4%, 38.9% and 38.4%, respectively. This enhancement was also statistically significant ($p < 0.05$) compared to the effect of low-dose IL-2 (18.1%), while their potentiating activity was comparable to that induced by the combination of ProTα and IL-2 (40.2%; Fig. 1). No statistically significant alterations in the percentage of specific lysis of either target was observed for PBMC activated with the remaining ProTα peptides, aa(98–109) to aa(94–109) or Ta1; in all cases mean % lysis did not exceed 16% and 26%, against K562 and Daudi targets, respectively (Fig. 1).

Table 1
Amino acid sequence of synthetic peptides spanning the ProTα C-terminus.

Peptide/amino acid position	Sequence
aa(103–109)	QKTDEDD
aa(102–109)	KQKTDEDD
aa(101–109)	KKQKTDEDD
aa(100–109)	TKKQKTDEDD
aa(99–109)	DTKKQKTDEDD
aa(98–109)	VDTKKQKTDEDD
aa(97–109)	DVDTKKQKTDEDD
aa(96–109)	DDVDTKKQKTDEDD
aa(95–109)	DDDVDTKKQKTDEDD
aa(94–109)	EDDDVDTKKQKTDEDD
aa(100–109)_scrambled	KETDKDKTDQ
aa(100–105)_NLS	TKKQKT
aa(1–28)	SDAAVDTSSEITTKDLKEKKEVVEEAEN

Primary structure of human ProTα: acSDAAVDTSSEITTKDLKEKKEVVEEAENGRDA PANGNANEENGEQEADNEVDEEEE EGGEEEEEEEEGDGEEEDGDEDEEAESATGKRAAE DDEDDDVDTKKQKTDEDD.
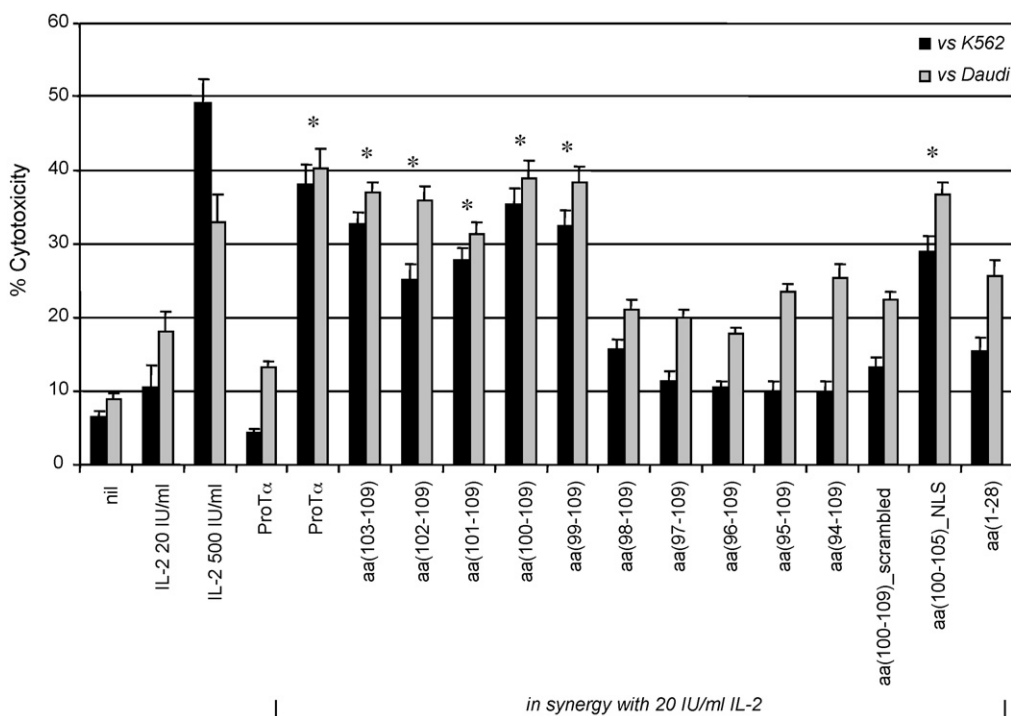
Fig. 1. Immunoenhancing synergistic effect of ProTα's C-terminal synthetic peptides with IL-2, on healthy donor-derived PBMC cytotoxicity. PBMC were incubated for 3 days with IL-2 (20 IU/ml) and the intact ProTα polypeptide (160 ng/ml) or each ProTα synthetic peptide (25 ng/ml), and tested as effectors against K562 and Daudi targets. In all experiments the E:T ratio was 40:1. Data are presented as mean % cytotoxicity ± SD from 12 volunteers. *$p < 0.05$ versus basal IL-2 stimulation (20 IU/ml).

The immunoreactivity mediated by the ProTα C-terminal synthetic peptides showed that the sequence aa(103–109) to aa(99–109) stimulates PBMC cytotoxicity, to levels similar to those induced by ProTα itself, with peptides aa(100–109) and aa(99–109) being the most potent. Examining the primary structure of the latter two revealed that prolonging the peptides' sequence from aa103 to aa100, resulted in the integration of the intact ProTα nuclear localization signal (NLS), namely TKKQKT (Marnow et al., 1991), within their primary structure. Thus, we synthesized and subsequently tested the immunoreactivity of two additional peptides (Table 1): (i) aa(100–109)_scrambled, KETDKDKTDQ, a peptide with the same amino acid composition as aa(100–109) but disrupted sequence, and ii) aa(100–105)_NLS, with sequence TKKQKT, in order to examine first, whether the specific primary structure of the NLS-containing aa(100–109) decapeptide dictates its immunoreactivity and second, whether the NLS sequence, by itself, represents the immunologically significant determinant for ProTα's C-terminal peptide activity.

Using a standard ^{51}Cr-release assay, we observed that only aa(100–105)_NLS, but not aa(100–109)_scrambled, augmented PBMC's NK and LAK cytotoxicity. Synergistically with low IL-2 dose, aa(100–109)_scrambled peptide resulted in K562 and Daudi target-lysis of 13.2% and 22.3%, respectively, while for aa(100–105)_NLS the respective values were 28.9% and 36.7% (Fig. 1). The activity of aa(100–105)_NLS was, in both assays, considered statistically significant ($p < 0.05$) compared to IL-2 (20 IU/ml), mimicking the activity of aa(100–109), aa(99–109) and of intact ProTα (Fig. 1), implying that the specific ProTα NLS sequence is necessary for triggering lymphocyte reactions.

3.2. Dendritic cell maturation

It is well established that the activity of ProTα is monocyte-dependent, in stimulating both CD4+ T cell proliferation, *via* increase in HLA-DR molecule expression, and NK cell lysis, *via* secretion of the pro-inflammatory cytokines TNF-α (Papanastasiou et al., 1992), IL-1β, IL-2 (Baxevanis et al., 1999) and IFN-γ (Qiu et al., 2002). This cytokine profile complies with a Th1-type polarization (Romagnani, 2000) and in conjunction with most recent data supporting a ProTα-mediated TLR signaling (Skopeliti et al., 2007), prompted us to investigate whether ProTα and its aa(100–109) active peptide influence dendritic cell maturation.

For this, we isolated monocytes from eight healthy donor-derived buffy coats and differentiated them *in vitro* into iDC, in the presence of GM-CSF and IL-4 for 6 days. On day 6, cells were activated with LPS, an agent known to cause DC maturation, ProTα, aa(100–109) or the aa(100–109)_scrambled peptide for 24–48 h. Immunophenotypic analyses for estimation of HLA-DR, CD80, CD83, CD86, CD11b, CD40 and CD14 surface molecule expression, were performed on days 6 and 7–8, to confirm the immature and/or mature status of DC, respectively.

As shown in Fig. 2 (black lines in all histograms), on day 6 harvested cells expressed intermediate levels of HLA-DR and CD11b (median fluorescence intensity (MFI) 156.4 and 73.7, respectively) and low levels of the co-stimulatory molecules CD80, CD86 and CD40 (MFI 36.1, 7.8 and 18.2, respectively) and the DC maturation marker CD83 (MFI 12.3). This DC immunophenotype, along with the low CD14 expression (MFI 22.3) compared to CD14 expression on day 0 (MFI 315.2; data not shown), indicated that by day 6 monocytes had differentiated into iDC (Fernandez-Ruiz et al., 2004; Pickl et al., 1996). iDC can efficiently uptake and process antigens, but show reduced antigen presenting abilities, related to low expression level of T-cell co-stimulatory molecules. Triggering iDC with pro-inflammatory mediators, e.g. TNF-α, IFN-γ or LPS, up-regulates the expression of surface molecules important for optimal antigen presentation and competent T-cell stimulation, such as HLA-DR, CD54, CD40, CD80, CD86 and CD83 (Corinti et al., 1999), whereas these cells completely lack CD14. Indeed, stimula-
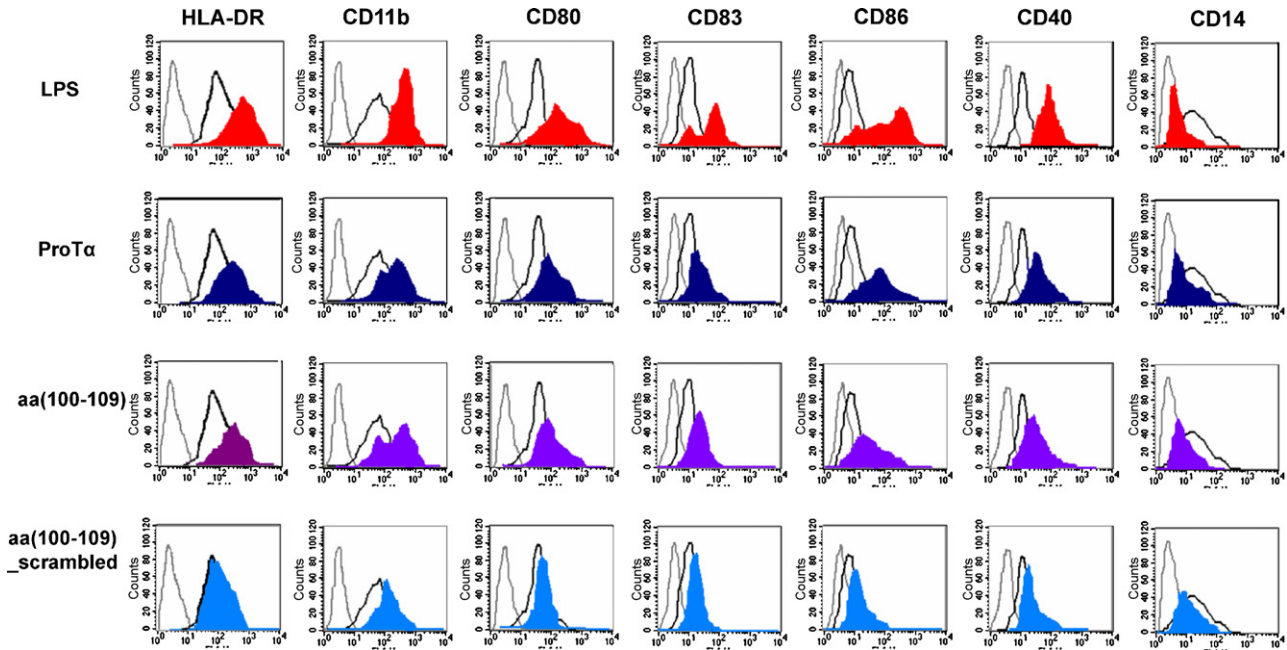
Fig. 2. HLA-DR, CD11b, CD80, CD86, CD83, CD40 and CD14 molecule expression of *in vitro* generated DC. CD14+ cells were cultured for 6 days in the presence of GM-CSF and IL-4, followed by 48 h exposure to LPS, ProTα, aa(100–109) or aa(100–109)_scrambled. Expression of mature DC surface markers was then determined by flow cytometry. The histograms shown are from one representative experiment of eight conducted. Filled colored histograms: mature DC; gray-line histograms: isotype controls; black-line histograms: immature DC. (For interpretation of the references to color in this figure legend, the reader is referred to the web version of the article.)

tion with LPS induced iDC to express, at relatively high-density, all these surface markers (MFI 533.2, 556.5, 225.6, 67.7, 115.6 and 103.4 for HLA-DR, CD11b, CD80, CD83, CD86 and CD40, respectively) and reduced CD14 expression (MFI 4.8; Fig. 2, filled histograms), thus confirming LPS ability to promote DC maturation (Willmann and Dunne, 2000).

In parallel, we activated iDC with ProTα, its immunoactive aa(100–109) or the aa(100–109)_scrambled peptide, and compared their phenotypes to LPS-matured DC. iDC activation with ProTα or aa(100–109) induced adequate expression of the afore mentioned DC surface markers, which followed a pattern resembling

that of LPS, albeit at lower levels (MFI 339.4, 229.8, 159.9, 27.1, 75.9 and 41.3 for ProTα- and 369.9, 354.3, 146.8, 22.1, 28.3 and 35.2 for aa(100–109)-induced HLA-DR, CD11b, CD80, CD83, CD86 and CD40, respectively; Fig. 2). In contrast, stimulation of iDC with aa(100–109)_scrambled did not sufficiently up-regulate HLA-DR, CD11b, CD80, CD83, CD86 and CD40 expression on iDC (MFI 215.1, 115.8, 85.7, 16.3, 14.1 and 23.5, respectively), supporting the sequence-specific activity of aa(100–109) and ProTα on DC maturation. Moreover, neither ProTα nor aa(100–109) peptide could substitute for GM-CSF and IL-4 administration in inducing monocyte differentiation to iDC upon a 6 day incubation (data not
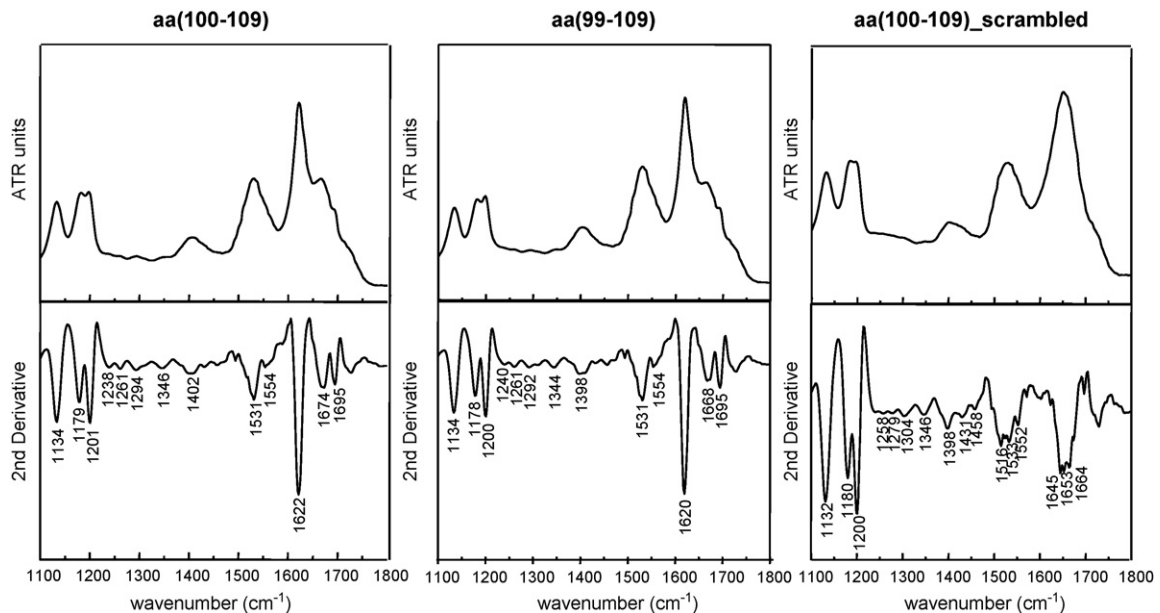

Fig. 3. ATR FT-IR spectra of ProTα's active C-terminal synthetic peptides aa(100–109) and aa(99–109) and the control peptide, aa(100–109)_scrambled. Second derivative spectra are also included.

Table 2
Amide I, II and III Infrared wavenumber ranges and their dependence on secondary structure and main ATR FT-IR band maxima of ProTα C-terminal peptides, as determined from the second derivative spectra.

Band	Secondary structure				ProTα's C-terminal peptides		
	α-Helix	β-Pleated sheet	β-Turns	Random/unordered	aa(100–109)	aa(99–109)	aa(100–109)_scrambled
Amide I	1644–1649[a] or 1653–1660[b]	1691–1699[a] and 1610–1640[a,b]	1662–1695[d]	1650–1654[a] or 1640–1650[b]	1695 1674 1622	1695 1668 1620	1664 1653 1645
Amide II	1548–1553[a] or 1519–1521[a]	1563[a] or 1530–1535[a]		1546–1553[a]	1554 1531	1554 1531	1552 1533 1516
Amide III	1280–1317[c]				1346 1294	1344 1292	1346 1304 1279 1258
				1245–1270[c]	1261	1261	
		1230–1245[c]			1238	1240	

[a] Venyaminov and Kalnin (1990).
[b] Griebenow et al. (1999).
[c] Singh et al. (1990).
[d] Orfanidou et al. (1995).

shown). Thus, both ProTα and its C-terminal peptide aa(100–109) are able to induce DC maturation, but not monocyte differentiation into iDC.

3.3. Structural characteristics of the ProTα's aa(100–109) active peptide

Having established that the NLS-containing aa(100–109) peptide, similarly to ProTα itself, triggers DC maturation and in order to elucidate the peptide's mode of action at the molecular level, we next investigated its structural characteristics by ATR FT-IR spectroscopy. Infrared spectroscopy collects vibrational spectra, which provide detailed information concerning a protein's secondary structure (Pelton and McLean, 2000). Attenuated total reflectance (ATR) FT-IR is usually applied to hydrated films of proteins or peptides, dictated by the need to exclude any possible spectroscopic and/or chemical interactions between the sample and the dispersing medium and eliminating saturation effects, which may be present in the transmission spectra of thicker samples. Thin films have been shown to maintain protein molecules in hydrated state and conserve their three-dimensional structure (Goormaghtigh et al., 1990). The ATR FT-IR spectra of ProTα's peptides aa(100–109), aa(99–109) and aa(100–109)_scrambled are presented in Fig. 3, together with their second derivative spectra.

Band inspection in the conformation-sensitive amide I, II and III regions (around 1600–1700 cm^{-1}, 1550–1600 cm^{-1} and 1220–1330 cm^{-1}, respectively) is generally employed to study protein structure. The structure-sensitive, strong amide I band originates mainly from carbonyl C=O stretching vibrations. For both, aa(100–109) and aa(99–109) peptides, bands appeared at 1622 and 1620 cm^{-1}, respectively, in the amide I region, suggesting that these peptides adopt β-sheet conformation (Venyaminov and Kalnin, 1990). The fact that these bands are rather sharp suggests a uniform secondary structure in the peptide films (Pelton and McLean, 2000). Interestingly, in the amide I region for both, aa(100–109) and aa(99–109) peptides, a shoulder at 1695 cm^{-1} also appears, which suggests an antiparallel β-sheet type of structure (Orfanidou et al., 1995 and refs. therein). The amide II band is mainly due to N–H bending coupled with C–N stretching. In this area, the finding of a band at 1531 cm^{-1}, observed for aa(100–109) and aa(99–109) peptides, is also an indication for the existence of a β-sheet structure (Griebenow et al., 1999). In agreement with the analysis of the amide I and II bands, the amide III band, which originates mainly

from C–N vibrations coupled with N–H in-plane bending vibrations, appears at 1238 cm^{-1} and 1240 cm^{-1} for aa(100–109) and aa(99–109) peptides, respectively, suggesting also the presence of a β-pleated sheet structure (Singh et al., 1990).

In contrast, the ATR FT-IR spectrum of the peptide aa(100–109)_scrambled (Fig. 3), as well as ProTα's aa(98–109) peptide (data not shown), do not exhibit similar bands, but rather bands indicating an unordered or random-coil structure. Wavenumbers of amide I, II and III bands for typical proteins with an α-helix, β-sheet, β-turn or random-coil conformation, as well as the ATR FT-IR band maxima of aa(100–109), aa(99–109) and aa(100–109)_scrambled peptides are shown in detail in Table 2.
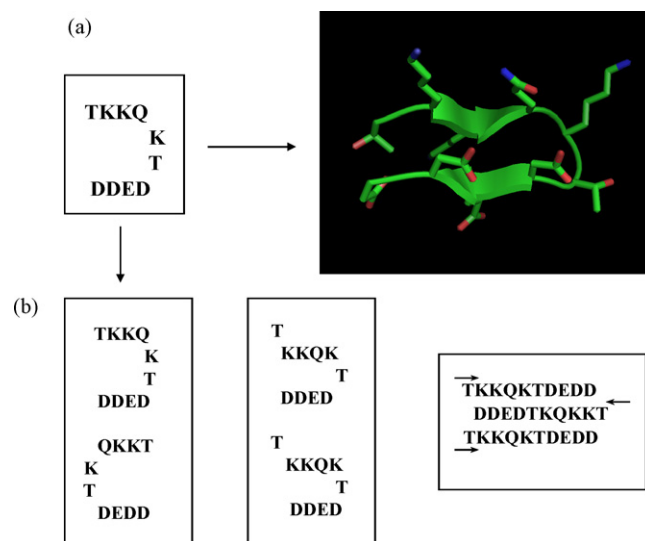

Fig. 4. ATR FT-IR data (Fig. 3 and Table 2) suggest an antiparallel β-pleated sheet structure for the aa(100–109) peptide. Schematically (a and b), various plausible antiparallel β-pleated sheet models and possible intermolecular arrangements are shown. Also, an antiparallel β-pleated sheet model structure ((a), right), for the aa(100–109) peptide is shown ((a), left), utilizing a ribbon representation (PyMOL, 2002, see Section 2), with the side chains of the amino acid residues shown as sticks. Arrows represent β-strands. View almost parallel to the β-pleated sheet surface. Neutralization of oppositely charged amino acid residues, resulting from favourable electrostatic interactions (salt bonds/ion pairs) of side chains of oppositely charged residues, might occur.
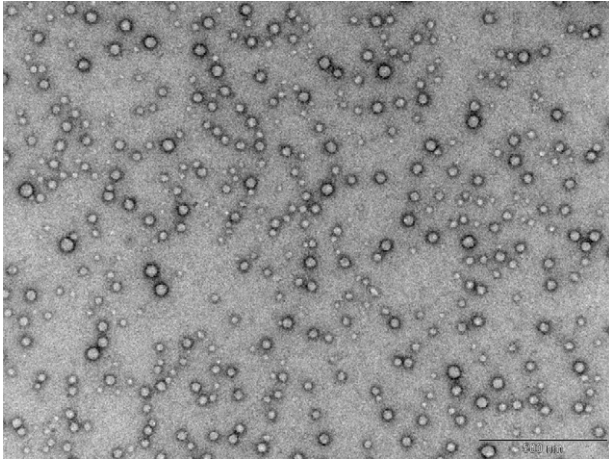
Fig. 5. Transmission electron micrograph of globular formations derived by self-assembly, after three weeks of incubation (this photograph), from a 5 mg/ml solution of the aa(100–109) peptide, in distilled H_2O, pH 5.5. The preparation was negatively stained with 1% uranyl acetate. Bar 500 nm.

Based on experimental information gathered from ATR FT-IR data from the C-terminal ProTα peptides, indicative of an antiparallel β-pleated sheet structure for aa(100–109) and aa(99–109) peptides, in conjunction with the fact that these peptides have a rather unusual primary structure dominated by the presence of a number of (consecutive) positively charged/polar lysine residues at the N-terminus (Table 1) followed by a number of (consecutive) negatively charged/polar aspartate and/or glutamate residues at the C-terminus, we constructed models, which may account for (a) the experimentally determined β-pleated sheet type of their structure and (b) the neutralization of oppositely charged amino acid residues, resulting from favourable electrostatic interactions (salt bonds/ion pairs) of side chains of oppositely charged residues. Some such plausible models are shown in Fig. 4.

Furthermore, we aimed to determine what sort (if any) of structure these peptides form in solution after self-assembly and aggregation. Since they adopt an antiparallel β-sheet type of structure, it was speculated that they might form amyloid-like fibrils. Therefore, solutions of peptide aa(100–109) at sufficient concentrations up to 5 mg/ml were made and after several days of incubation were negatively stained and visualized by transmission electron microscopy. Only globular formations, ca. 15–60 nm in diameter, in various aggregation classes could be identified in the negatively stained preparations (Fig. 5) and these findings remained systematically the same, independent of pH variation (data not shown). Thus, there was no evidence for the existence of amyloid-like fibrils.

4. Discussion

ProTα was initially isolated as the precursor molecule of the immunostimulatory Tα1-related peptides (Haritos et al., 1984). However, it was shown to be more effective in stimulating various leukocyte reactions than other members of the α-thymosin family (Haritos, 1987). Accumulating evidence yet attributes a different, albeit equally significant, role to ProTα. The polypeptide sustains nuclear events related to stimulation of cell proliferation (Karetsou et al., 1998) and regulation of apoptosis (Piacentini et al., 2003). This dual role has caused reluctance to use ProTα to treat immunodeficiencies. However, if, along the polypeptide's backbone, ProTα's immunological centre extended to an area distinct from ProTα's histone-binding segment which mediates its intracellular effects (Rodriguez et al., 1998), then the former peptide sequence would have advantages for clinical application; thus the risk of sustaining pathological cell growth if transported to the nucleus would be reduced. There would also be a practical advantage in that production would be easier due to its smaller mass.

Based on previous data, in which we showed that the immunoactive ProTα segment spans aa(89–109) (Skopeliti et al., 2006), in the present study we aimed to precisely identify the relevant sequence that could substitute the immunoenhancing activity of the intact molecule and to determine which of its characteristics are of significance for lymphocyte stimulation. Therefore, we evaluated the ability of longer synthetic peptides spanning the C-terminal sequence of ProTα and appropriate control peptides, to up-regulate NK and LAK cell cytotoxicity, as well as lymphocyte proliferation in response to autologous antigens (data not shown), functionalities that have been extensively used to explore the activity of ProTα (Baxevanis et al., 1988, 1999) and its active fragments (Haritos, 1987; Skopeliti et al., 2006). Herein, we identified peptides aa(100–109) and aa(99–109) as the most immunologically potent, exhibiting a sequence-specific activity, similar to intact ProTα. These findings support our initial hypothesis, i.e., the immunologically significant determinant(s) of ProTα are localized distinctly apart from its central, energy-rich histone-binding sequence aa(52–82) (Papamarkaki and Tsolas, 1994) and can be solely addressed to the action of its C-terminus, a segment until now considered important only for the polypeptide's nuclear targeting (Manrow et al., 1991). However, they are not consistent with evidence supporting the idea that the N-terminal segment aa(1–28), otherwise termed Tα1, is the functionally active ProTα area, although, both *in vitro* and *in vivo*, Tα1 is systematically reported to exert its activity at much higher concentrations than ProTα on an equimolar basis (Haritos, 1987; Pica et al., 1998). Nevertheless, such reports have facilitated the entry of Tα1, under the trade name Zadaxin, into clinical trials for the treatment of chronic hepatitis B and hepatitis C virus infections and non-small cell lung cancer (Garaci, 2007).

An important issue that was of particular significance regarding the sequence of the most active peptide aa(100–109) was that it included the intact undisrupted NLS, comprised of amino acids TKKQKT (Manrow et al., 1991). By additionally testing the activity of the peptide aa(100–105)_NLS, shown to be immunologically active, although less than aa(100–109), we propose that the lysine-rich NLS motif, included either intact or partially within the peptides' sequence, contributes to lymphocyte stimulation. This supports our earlier observation on the identification of two ProTα active C-terminal fragments, both of which contained part of the NLS sequence (TKK–QKT; Skopeliti et al., 2006) and indicates that the C-terminal ProTα residues, namely DEDD, are also important for optimal lymphocyte activation, since the reactivity of the decapeptide TKKQKTDEDD is higher and similar to that of intact ProTα. Our data, in conjunction with reports revealing a mechanism of ProTα truncation (Evstafieva et al., 2000, 2003; Enkemann et al., 2000), suggest that this *in vivo* generated C-terminal fragmentation product of ProTα is of immunological importance.

To further elucidate the mode of action of the aa(100–109) segment, in conjunction with the established monocyte-dependent activity of ProTα (Baxevanis et al., 1988) and its ability to signal downstream TLR (Skopeliti et al., 2007), we investigated whether ProTα and its active peptide evoke DC maturation. We found that neither ProTα nor any of the peptides mediated the differentiation of monocytes into iDC (data not shown), but exposing iDC to ProTα or aa(100–109) resulted in increased HLA-DR, CD80, CD83, CD86, CD40 and CD11b expression, i.e., acquisition of a mature DC immunophenotype, competent for strong T-cell stimulation (Banchereau et al., 2000). This observation supports ProTα and aa(100–109) peptide's potential in stimulating the mixed lymphocyte reaction and the secretion of pro-inflammatory cytokines such

as TNF-α (Papanastasiou et al., 1992; Skopeliti et al., in preparation), IL-1β, IL-2 (Baxevanis et al., 1999) and IFN-γ (Qiu et al., 2002), towards Th1 polarization (Romagnani, 2000) and subsequent increase of NK cytotoxicity (Smyth et al., 2005).

DC maturation *in vivo* is provoked by infectious and/or endogenous signals derived from pathogens, damaged-tissue mediators, or pro-inflammatory cytokines (Matzinger, 1994). TLR engagement is one of the dominant pathways in DC triggering, as TLR can recognize a remarkable variety of structures endowed with pro-inflammatory properties, e.g. unmethylated CpG islands or bacterial and viral DNA, single or double stranded RNA, heat shock proteins and extracellular-matrix breakdown products (Gallucci and Matzinger, 2001; Beg, 2002; Miyake, 2007). In this respect, it would be of interest to determine whether ProTα's NLS-containing aa(100–109) acquires a specific secondary conformation in solution. By ATR FT-IR spectrometry, we showed that aa(100–109) polymerizes into β-pleated sheets, the core structure of amyloid fibrils (Hiramatsu et al., 2005). We therefore propose a model on aa(100–109) polymerization: the specific primary sequence of the peptide generates oppositely charged N- and C-termini, and practically the peptide aa(100–109) forms an heteropole. Consequently, electrostatic interactions stabilize juxtaposed peptide monomers to form antiparallel β-sheets. This explains why disruption (peptide aa(100–109_scrambled)), shortening (peptides aa(101–109) or elongation (peptides aa(98–109) to aa(94–109)) of the specific primary structure of aa(100–109), although in the latter peptides ProTα's NLS is still included, results in reduced immunological activity of the segments.

Proteins misfolded and/or aggregated into amyloid-like fibrils, e.g. Aβ peptide (Buchete and Hummer, 2007), β2-microglobulin (Zheng et al., 2008) or macrophage migration inhibitory factor (Lashuel et al., 2005) are known to exert a pro-inflammatory activity, most probably *via* TLR (Lotz et al., 2005). Among other intracellular proteins (Lee et al., 2003), ProTα was also reported to form amyloid fibrils around its isoelectric point (Pavlov et al., 2002), but our electron microscopy studies, independently of any pH used, did not reveal the formation of an amyloid-like fibril structure for the active TKKQKTDEDD peptide. Nevertheless, our structural analysis provides strong data in favour of the ability of peptide aa(100–109) to form antiparallel β-sheet structures, which may nucleate and probably act as a seeding sequence of the reported amyloid fibril formation by ProTα (Pavlov et al., 2002).

In summary, the results presented here suggest that ProTα's C-terminal aa(100–109) active peptide exhibits a pro-inflammatory activity in stimulating immune responses, being able to induce DC maturation, adopting a β-sheet conformation in a sequence-specific manner. Data in the literature on ProTα's *in vivo* targeting during apoptosis, indicate a major cleavage site for caspase-3 and -7 at D[99] (Evstafieva et al., 2000), indicating the conditions under which the peptide aa(100–109) is generated. Intriguingly, while ProTα aa(1–99) lacking the NLS is relocalized and consequently detected in the cytoplasm, ProTα's C-terminal peptide aa(100–109) has still not been identified either in the nucleus or the cytoplasm (Evstafieva et al., 2000, 2003).

In line with these data and in an attempt to describe an *in vivo* mechanism for the production and action of ProTα's active site, our present findings strengthen our earlier hypothesis on ProTα's dual mode of action, immunological and intracellular, as follows. ProTα, like other strictly cytoplasmic (e.g. HSP90; Basu et al., 2000) and nuclear, histone-binding (e.g. HMGB1; Rovere-Querini et al., 2004; Scaffidi et al., 2002) proteins, if released extracellularly or excreted from cells *via* yet unknown mechanisms, acts as an adjuvant *via* antigen presenting cells, such as monocytes and DC (Messmer et al., 2004), downstream TLR stimulation (Tsung et al., 2005; Tian et al., 2007), triggering both innate and adaptive immune responses.

Extracellular release of cell-contents is reported to occur during necrosis (El Mezayen et al., 2007), as well as during programmed cell death, e.g. apoptosis upon noxious agent insults (Bell et al., 2006; Fink and Cookson, 2005; DeLeo, 2004). In the latter case, the ProTα TKKQKTDEDD peptide is produced *in vivo* on early stage caspase activation and subsequently polymerizes into β-pleated sheet structures, thus being protected from further degradation (Lee et al., 2007; Skopeliti et al., in preparation). Compared to amyloid fibrils sedimenting in the cytoplasm, ProTα aa(100–109) peptide may be, actively or passively, excreted from dying cells and hence provide a danger signal to iDC, stimulating the commencement of lymphocyte immune reactions.

Acknowledgements

References

Bancherau, J., Briere, F., Caux, C., Davoust, J., Lebecque, S., Liu, Y.J., Pulendran, B., Palucka, K., 2000. Immunobiology of dendritic cells. Annu. Rev. Immunol. 18, 767–811.

Basu, S., Binder, R.J., Suto, R., Anderson, K.M., Srivastava, P.K., 2000. Necrotic but not apoptotic cell death releases heat shock proteins, which deliver a partial maturation signal to dendritic cells and activate the NF-kappa B pathway. Int. Immunol. 12, 1539–1546.

Baxevanis, C.N., Reclos, G.J., Panneerselvam, C., Papamichail, M., 1988. Enhancement of human T lymphocyte functions by prothymosin alpha. I. Augmentation of mixed lymphocyte culture reactions and soluble protein-induced proliferative responses. Immunopharmacology 15, 73–84.

Baxevanis, C.N., Spanakos, G., Voutsas, I.F., Gritzapis, A.D., Tsitsilonis, O.E., Mamalaki, A., Papamichail, M., 1999. Increased generation of autologous tumor-reactive lymphocytes by anti-CD3 monoclonal antibody and prothymosin alpha. Cancer Immunol. Immunother. 48, 71–84.

Baxevanis, C.N., Thanos, D., Reclos, G.J., Anastasopoulos, E., Tsokos, G.C., Papamatheakis, J., Papamichail, M., 1992. Prothymosin alpha enhances human and murine MHC class II surface antigen expression and messenger RNA accumulation. J. Immunol. 148, 1979–1984.

Beg, A.A., 2002. Endogenous ligands of Toll-like receptors: implications for regulating inflammatory and immune responses. Trends Immunol. 23, 509–512.

Bell, C.W., Jiang, W., Reich 3rd, C.F., Pisetsky, D.S., 2006. The extracellular release of HMGB1 during apoptotic cell death. Am. J. Physiol. Cell Physiol. 291, C1318–1325.

Berman, H.M., Westbrook, J., Feng, Z., Gilliland, G., Bhat, T.N., Weissig, H., Shindyalov, I.N., Bourne, P.E., 2000. The Protein Data Bank. Nucleic Acids Res. 28, 235–242.

Buchete, N.V., Hummer, G., 2007. Structure and dynamics of parallel β-sheets, hydrophobic core, and loops in Alzheimer's Aβ fibrils. Biophys. J. 92, 3032–3039.

Cordero, O.J., Sarandeses, C., López-Rodríguez, J.L., Nogueira, M., 1995. The presence and cytotoxicity of CD16+ CD2-subset from PBL and NK cells in long-term IL-2 cultures enhanced by Prothymosin-alpha. Immunopharmacology 29, 215–223.

Corinti, S., Fanales-Belasio, E., Albanesi, C., Cavani, A., Angelisova, P., Girolomoni, G., 1999. Cross-linking of membrane CD43 mediates dendritic cell maturation. J. Immunol. 162, 6331–6336.

DeLano, W.L., 2002. The PyMOL Molecular Graphics System, DeLano Scientific, Palo Alto, CA, US (http://www.pymol.org).

DeLeo, F.R., 2004. Modulation of phagocyte apoptosis by bacterial pathogens. Apoptosis 9, 399–413.

Díaz-Jullien, C., Perez-Estevez, A., Covelo, G., Freire, M., 1996. Prothymosin alpha binds histones in vitro and shows activity in nucleosome assembly assay. Biochim. Biophys. Acta 1296, 219–227.

Eckert, C., Grünberg, E., Immenschuh, P., Garbin, F., Kreuser, E.D., Maurer, H.R., 1997. Interleukin-2-activated killer cell activity in colorectal tumor patients: evaluation of in vitro effects by prothymosin alpha1. J. Cancer Res. Clin. Oncol. 123, 420–428.

El Mezayen, R., El Gazzar, M., Seeds, M.C., McCall, C.E., Dreskin, S.C., Nicolls, M.R., 2007. Endogenous signals released from necrotic cells augment inflammatory responses to bacterial endotoxin. Immunol. Lett. 111, 36–44.

Enkemann, S.A., Wang, R.H., Trumbore, M.W., Berger, S.L., 2000. Functional discontinuities in prothymosin alpha caused by caspase cleavage in apoptotic cells. J. Cell. Physiol. 182, 256–268.

Eschenfeldt, W.H., Berger, S.L., 1986. The human prothymosin alpha gene is polymorphic and induced upon growth stimulation: evidence using a cloned cDNA. Proc. Natl. Acad. Sci. U.S.A. 83, 9403–9407.

Evstafieva, A.G., Belov, G.A., Kalkum, M., Chichkova, N.V., Bogdanov, A.A., Agol, V.I., Vartapetian, A.B., 2000. Prothymosin alpha fragmentation in apoptosis. FEBS Lett. 467, 150–154.

Evstafieva, A.G., Belov, G.A., Rubtsov, Y.P., Kalkum, M., Joseph, B., Chichkova, N.V., Sukhacheva, E.A., Bogdanov, A.A., Pettersson, R.F., Agol, V.I., Vartapetian, A.B., 2003. Apoptosis-related fragmentation, translocation and properties of human prothymosin alpha. Exp. Cell Res. 284, 211–223.

Fernandez-Ruiz, V., Gonzalez, A., Lopez-Moratalla, N., 2004. Effect of nitric oxide in the differentiation of human monocytes to dendritic cells. Immunol. Lett. 93, 87–95.

Fink, S.L., Cookson, B.T., 2005. Apoptosis, pyroptosis, and necrosis: mechanistic description of dead and dying eukaryotic cells. Infect. Immun. 73, 1907–1916.

Gallucci, S., Matzinger, P., 2001. Danger signals: SOS to the immune system. Curr. Opin. Immunol. 13, 114–119.

Garaci, E., 2007. Thymosin alpha1: a historical overview. Ann. NY Acad. Sci. 1112, 14–20.

Garbin, F., Eckert, K., Immenschuh, P., Kreuser, E.D., Maurer, H.R., 1997. Prothymosin alpha 1 effects, in vitro, on the antitumor activity and cytokine production of blood monocytes from colorectal tumor patients. Int. J. Immunopharmacol. 19, 323–332.

Gomez-Marquez, J., Segade, F., Dosil, M., Pichel, J.G., Bustelo, X.R., Freire, M., 1989. The expression of prothymosin alpha gene in T lymphocytes and leukemic lymphoid cells is tied to lymphocyte proliferation. J. Biol. Chem. 264, 8451–8454.

Goormaghtigh, E., Cabiaux, V., Ruysschaert, J.M., 1990. Secondary structure and dosage of soluble and membrane proteins by attenuated total reflection Fourier-transform infrared spectroscopy on hydrated films. Eur. J. Biochem. 193, 409–420.

Griebenow, K., Santos, A.M., Carrasquillo, K.G., 1999. Secondary structure of proteins in the amorphous dehydrated state probed by FT-IR spectroscopy. Dehydration-induced structural changes and their prevention. Inter. J. Vibr. Spectr. 3, 1–34.

Haritos, A.A., 1987. Alpha-thymosins: relations in structure, distribution and function. In: Rattazzi, M., Scandalios, J., Whitt, G. (Eds.), Isozymes: Current Topics in Biological and Medical Research, vol. 14. Alan R. Liss, Inc., pp. 123–152.

Haritos, A.A., Goodall, G.J., Horecker, B.L., 1984. Prothymosin alpha: isolation and properties of the major immunoreactive form of thymosin alpha 1 in rat thymus. Proc. Natl. Acad. Sci. U.S.A. 81, 1008–1011.

Heidecke, H., Eckert, K., Schulze-Forster, K., Maurer, H.R., 1997. Prothymosin alpha 1 effects in vitro on chemotaxis, cytotoxicity and oxidative response of neutrophils from melanoma, colorectal and breast tumor patients. Int. J. Immunopharmacol. 19, 413–420.

Hiramatsu, H., Goto, Y., Naiki, H., Kitagawa, T., 2005. Structural model of the amyloid fibril formed by β(2)-microglobulin #21-31 fragment based on vibrational spectroscopy. J. Am. Chem. Soc. 127, 7988–7999.

Jiang, X., Kim, H.E., Shu, H., Zhao, Y., Zhang, H., Kofron, J., Donnelly, J., Burns, D., Ng, S.C., Rosenberg, S., Wang, X., 2003. Distinctive roles of PHAP proteins and prothymosin-alpha in a death regulatory pathway. Science 299, 223–226.

Karetsou, Z., Kretsovali, A., Murphy, C., Tsolas, O., Papamarcaki, T., 2002. Prothymosin alpha interacts with the CREB-binding protein and potentiates transcription. EMBO Rep. 3, 361–366.

Karetsou, Z., Sandaltzopoulos, R., Frangou-Lazaridis, M., Lai, C.Y., Tsolas, O., Becker, P.B., Papamarcaki, T., 1998. Prothymosin alpha modulates the interaction of histone H1 with chromatin. Nucleic Acids Res. 26, 3111–3118.

Lashuel, H.A., Aljabari, B., Sigurdsson, E.M., Metz, C.N., Leng, L., Callaway, D.J., Bucala, R., 2005. Amyloid fibril formation by macrophage migration inhibitory factor. Biochem. Biophys. Res. Commun. 338, 973–980.

Lee, A.S., Galea, C., DiGiammarino, E.L., Jun, B., Murti, G., Ribeiro, R.C., Zambetti, G., Schultz, C.P., Kriwacki, R.W., 2003. Reversible amyloid formation by the p53 tetramerization domain and a cancer-associated mutant. J. Mol. Biol. 327, 699–709.

Lee, S., Fernandez, E.J., Good, T.A., 2007. Role of aggregation conditions in structure, stability, and toxicity of intermediates in the Aβ fibril formation pathway. Protein Sci. 16, 723–732.

Lopez-Rodriguez, J.L., Cordero, O.J., Sarandeses, C., Vinuela, J., Nogueira, M., 1994. Interleukin-2 killer cells: in vitro evaluation of combination with prothymosin alpha. Lymphokine Cytokine Res. 13, 175–182.

Lotz, M., Ebert, S., Esselmann, H., Iliev, A.I., Prinz, M., Wiazewicz, N., Wiltfang, J., Gerber, J., Nau, R., 2005. Amyloid β peptide 1-40 enhances the action of Toll-like receptor-2 and -4 agonists but antagonizes Toll-like receptor-9-induced inflammation in primary mouse microglial cell cultures. J. Neurochem. 94, 289–298.

Manrow, R.E., Sburlati, A.R., Hanover, J.A., Berger, S.L., 1991. Nuclear targeting of prothymosin alpha. J. Biol. Chem. 266, 3916–3924.

Markova, O.V., Evstafieva, A.G., Mansurova, S.E., Moussine, S.S., Palamarchuk, L.A., Pereverzev, M.O., Vartapetian, A.B., Skulachev, V.P., 2003. Cytochrome c is transformed from anti- to pro-oxidant when interacting with truncated oncoprotein prothymosin alpha. Biochim. Biophys. Acta 1557, 109–117.

Matzinger, P., 1994. Tolerance, danger, and the extended family. Annu. Rev. Immunol. 12, 991–1045.

Messmer, D., Yang, H., Telusma, G., Knoll, F., Li, J., Messmer, B., Tracey, K.J., Chiorazzi, N., 2004. High mobility group box protein 1: an endogenous signal for dendritic cell maturation and Th1 polarization. J. Immunol. 173, 307–313.

Miyake, K., 2007. Innate immune sensing of pathogens and danger signals by cell surface Toll-like receptors. Semin. Immunol. 19, 3–10.

Orfanidou, C.C., Hamodrakas, S.J., Chryssikos, G.D., Kamitsos, E.I., Wellman, S.E., Case, S.T., 1995. Spectroscopic studies of *Manduca sexta* and Sesamia nonagrioides chorion protein structure. Int. J. Biol. Macromol. 17, 93–98.

Pan, L.X., Haritos, A.A., Wideman, J., Komiyama, T., Chang, M., Stein, S., Salvin, S.B., Horecker, B.L., 1986. Human prothymosin alpha: amino acid sequence and immunologic properties. Arch. Biochem. Biophys. 250, 197–201.

Papamarcaki, T., Tsolas, O., 1994. Prothymosin alpha binds to histone H1 in vitro. FEBS Lett. 345, 71–75.

Papanastasiou, M., Baxevanis, C.N., Papamichail, M., 1992. Promotion of murine antitumor activity by prothymosin alpha treatment: I. Induction of tumoricidal peritoneal cells producing high levels of tumour necrosis factor alpha. Cancer Immunol. Immunother. 35, 145–150.

Pavlov, N.A., Cherny, D.I., Heim, G., Jovin, T.M., Subramaniam, V., 2002. Amyloid fibrils from the mammalian protein prothymosin alpha. FEBS Lett. 517, 37–40.

Pelton, J.T., McLean, L.R., 2000. Spectroscopic methods for analysis of protein secondary structure. Anal. Biochem. 277, 167–176.

Piacentini, M., Evangelisti, C., Mastroberardino, P.G., Nardacci, R., Kroemer, G., 2003. Does prothymosin-alpha act as molecular switch between apoptosis and autophagy? Cell Death Differ. 10, 937–939.

Pica, F., Fraschetti, M., Matteucci, C., Tuthill, C., Rasi, G., 1998. High doses of thymosin alpha 1 enhance the anti-tumor efficacy of combination chemo-immunotherapy for murine B16 melanoma. Anticancer Res. 18, 3571–3578.

Pickl, W.F., Majdic, O., Kohl, P., Stöckl, J., Riedl, E., Scheinecker, C., Bello-Fernandez, C., Knapp, W., 1996. Molecular and functional characteristics of dendritic cells generated from highly purified CD14+ peripheral blood monocytes. J. Immunol. 157, 3850–3859.

Qiu, L., Guo, B.Y., Miao, H., Dao, S.Y., Zhang, R., Yuan, P.Q., Yang, X., 2002. Effect of recombinant prothymosin alpha on secretion of IFN-gamma, IFN-alpha and TNF-alpha in vitro. Yao Xue Xue Bao 37, 326–328.

Reclos, G.J., Baxevanis, C.N., Sfagos, C., Papageorgiou, C., Tsokos, G.C., Papamichail, M., 1987. Multiple sclerosis: II. Effects of prothymosin alpha on the autologous and allogeneic MLR in patients with multiple sclerosis. Clin. Exp. Immunol. 70, 336–344.

Rodriguez, P., Vinuela, J.E., Alvarez-Fernandez, L., Buceta, M., Vidal, A., Dominguez, F., Gomez-Marquez, J., 1998. Overexpression of prothymosin alpha accelerates proliferation and retards differentiation in HL-60 cells. Biochem. J. 331, 753–761.

Romagnani, S., 2000. T-cell subsets (Th1 versus Th2). Ann. Allergy Asthma Immunol. 85, 9–18.

Rovere-Querini, P., Capobianco, A., Scaffidi, P., Valentinis, B., Catalanotti, F., Giazzon, M., Dumitriu, I.E., Müller, S., Iannacone, M., Traversari, C., Bianchi, M.E., Manfredi, A.A., 2004. HMGB1 is an endogenous immune adjuvant released by necrotic cells. EMBO Rep. 5, 825–830.

Savitsky, A., Golay, M.J.E., 1964. Smoothing and differentiation of data by simplified least-squares procedures. Anal. Chem. 36, 1627–1639.

Scaffidi, P., Misteli, T., Bianchi, M.E., 2002. Release of chromatin protein HMGB1 by necrotic cells triggers inflammation. Nature 418, 191–195.

Singh, B.R., Fuller, M.P., Schiavo, G., 1990. Molecular structure of tetanus neurotoxin as revealed by Fourier transform infrared and circular dichroic spectroscopy. Biophys. Chem. 36, 155–166.

Skopeliti, M., Kratzer, U., Altenberend, F., Panayotou, G., Kalbacher, H., Stevanovic, S., Voelter, W., Tsitsilonis, O.E., 2007. Proteomic exploitation on prothymosin alpha-induced mononuclear cell activation. Proteomics 7, 1814–1824.

Skopeliti, M., Voutsas, I.F., Klimentzou, P., Tsiatas, M.L., Beck, A., Bamias, A., Moraki, M., Livaniou, E., Neagu, M., Voelter, W., Tsitsilonis, O.E., 2006. The immunologically active site of prothymosin alpha is located at the carboxy-terminus of the polypeptide. Evaluation of its in vitro effects in cancer patients. Cancer Immunol. Immunother. 55, 1247–1257.

Smyth, M.J., Cretney, E., Kelly, J.M., Westwood, J.A., Street, S.E., Yagita, H., Takeda, K., van Dommelen, S.L., Degli-Esposti, M.A., Hayakawa, Y., 2005. Activation of NK cell cytotoxicity. Mol. Immunol. 42, 501–510.

Tian, J., Avalos, A.M., Mao, S.Y., Chen, B., Senthil, K., Wu, H., Parroche, P., Drabic, S., Golenbock, D., Sirois, C., Hua, J., An, L.L., Audoly, L., La Rosa, G., Bierhaus, A., Naworth, P., Marshak-Rothstein, A., Crow, M.K., Fitzgerald, K.A., Latz, E., Kiener, P.A., Coyle, A.J., 2007. Toll-like receptor 9-dependent activation by DNA-containing immune complexes is mediated by HMGB1 and RAGE. Nat. Immunol. 8, 487–496.

Tsung, A., Sahai, R., Tanaka, H., Nakao, A., Fink, M.P., Lotze, M.T., Yang, H., Li, J., Tracey, K.J., Geller, D.A., Billiar, T.R., 2005. The nuclear factor HMGB1 mediates hepatic injury after murine liver ischemia-reperfusion. J. Exp. Med. 201, 1135–1143.

Venyaminov, S.Y., Kalnin, N.N., 1990. Quantitative IR spectrophotometry of peptide compounds in water (H_2O) solutions. II. Amide absorption bands of polypeptides and fibrous proteins in alpha-, β-, and random coil conformations. Biopolymers 30, 1259–1271.

Vriend, G., 1990. WHAT IF: a molecular modeling and drug design program. J. Mol. Graph. 8, 52–56.

Voutsas, I.F., Baxevanis, C.N., Gritzapis, A.D., Missitzis, I., Stathopoulos, G.P., Archodakis, G., Banis, C., Voelter, W., Papamichail, M., 2000. Synergy between interleukin-2 and prothymosin alpha for the increased generation of cytotoxic T lymphocytes against autologous human carcinomas. Cancer Immunol. Immunother. 49, 449–458.

Willmann, K., Dunne, J.F., 2000. A flow cytometric immune function assay for human peripheral blood dendritic cells. J. Leukoc. Biol. 67, 536–544.

Zheng, J., Jang, H., Nussinov, R., 2008. β(2)-Microglobulin amyloid fragment organization and morphology and its comparison to Aβ suggests that amyloid aggregation pathways are sequence specific. Biochemistry 47, 2497–2509.